A Particle Swarm Optimization Algorithm With Novel Expected Fitness Evaluation for Robust Optimization Problems

Feng Luan[1,2], Jong-Ho Choi[1], and Hyun-Kyo Jung[1]

[1]School of Electrical Engineering and Computer Science, Seoul National University, Seoul 151-744, Korea
[2]College of Information Science and Engineering, Northeastern University, Shenyang, 110819, China

In this paper, an improved particle swarm optimization (PSO) algorithm for robust optimization problems is proposed. The new algorithm, named robust particle swarm optimization (RPSO), deeps basic concepts of the PSO, results in dynamic determination of the robust optimal solution by using a 2^n-quadrant-longest-distance expected fitness evaluation strategy in n-D space, and obtains robustness against the perturbation of design variables. The efficiency and advantages of the proposed algorithm are verified by the application to a mathematical function and a practical electromagnetic problem.

***Index Terms*—Dielectric configuration, electromagnetic scattering, expected fitness, PSO, robust optimal design.**

I. Introduction

In 1995, a stochastic optimization strategy named particle swarm optimization (PSO) was originally proposed by Eberhart and Kennedy inspired by the social behavior associated with swarm of bees [1]. The underlying mechanism of PSO is that, particles move through the problem space influenced by the optimum experience of individual (pbest) and swarm (gbest) simultaneously [2]. Traditionally, the ultimate attempt of PSO is to find one global or several local optimal solution(s) [3], [4].

PSO has been proved to be a successful tool used to solve many difficult optimization problems [5]–[7]. While these works demonstrate the advantage of PSO, most PSO methods assume that the design variables are stable and do not suffer any errors, therefore, these PSO algorithms do not provide solutions that are intrinsically robust against errors. Robust optimization design implies that the optimal solution should be able to tolerate the small perturbations or slight variations of the design variables [8]–[10]. Therefore, the robustness of the optimization solutions still remains an open issue, and taking perturbations into account during the optimization process is of interest to engineers [11]–[13].

In this paper, an algorithm named robust particle swarm optimization (RPSO) is proposed in order to search the robust optimal solution of an inverse problem as well as preserve the advantages of available PSO algorithms. A key characteristic of our work is that it develops a detailed process of robust PSO with a 2^n-quadrant-longest-distance expected fitness evaluation strategy. Previous works of PSO did not take into account variable errors that can lead to infeasible solutions. The RPSO method inherently improves the robustness of the optimized solution with respect to perturbation of design variables. The feasibility of the RPSO is demonstrated by application to a mathematical function and a practical electromagnetic problem.

Manuscript received July 03, 2011; revised October 10, 2011; accepted October 22, 2011. Date of current version January 25, 2012. Corresponding author: F. Luan (e-mail: luanfeng1979@hotmail.com)

Color versions of one or more of the figures in this paper are available online at http://ieeexplore.ieee.org.

Digital Object Identifier 10.1109/TMAG.2011.2173753

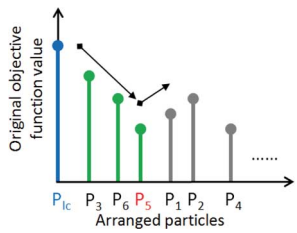

Fig. 1. A schematic illustration of the candidate selection in one quadrant.

II. Proposed Algorithm

A. Initialization (Step 1)

Define the search space and the swarm population size, and generate the particles' locations and velocities randomly.

B. Update Position and Refresh Candidate Pool (Step 2)

The position of a particle is determined based on the current location and velocity, then the object function is calculated for each updated particle, the particle with best value of the original objective function is defined as leading candidate $(\mathrm{P_{lc}})$.

C. Evaluate Expected Fitness (Step 3)

Here, a 2^n-quadrant-longest-distance method is introduced to evaluate the robust performance of an optimal solution. The n-D search space is divided into 2^n-quadrant by using the $\mathrm{P_{lc}}$ as the origin in the n-D coordinate system, the point (0, 0) in the case of 2-D search space. Next, in each quadrant, the particles are arranged in ascending order according to the distance they are from the leading candidate. The criterion for the arranged particles to become feasible for evaluating the robust performance is that the original objective function values of the feasible particles should always be in descending order. Fig. 1 shows the particles after arrangement in one of the quadrants. $\mathrm{P_3}$, $\mathrm{P_6}$, and $\mathrm{P_5}$ are feasible particles because their objective function values decline with increasing distance from $\mathrm{P_{lc}}$. The descending trend is broken by $\mathrm{P_1}$ since the objective function value of $\mathrm{P_1}$ is higher than that of $\mathrm{P_5}$. Once the descending trend is ended, the feasible particle with the longest-distance from $\mathrm{P_{lc}}$ is defined as common candidate, i.e., the $\mathrm{P_5}$ in Fig. 1.

0018-9464/$31.00 © 2012 IEEE

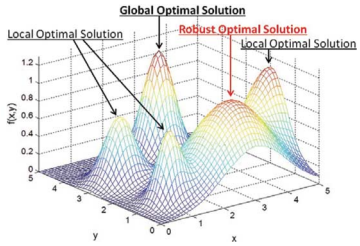

Fig. 2. The test function.

Obviously, there are at most 2^n common candidates in the n-D space. In 2-D space, there are at most four common candidates that will be used in robust performance evaluation. The novelty of the 2^n-quadrant-longest-distance strategy is that the condition for particles to be selected for evaluating the robust performance is not limited to a predefined small region around the solution in question [9], [14], hence, alleviating the computation burden for generating additional particles. It is conceivable that the spread range of a robust optimal solution is greater than that of a conventional optimal solution. Thus, function $R(\cdot)$ is proposed to indicate the spread of an optimal solution. The value of $R(\cdot)$ for a solution with the larger spread range is greater. Based on this indication, we can evaluate the robust performance of a solution using the following expected fitness function

$$f_{\exp}(x,y) = f_{\mathrm{o}}(x,y) \cdot [R(x,y)]^{\beta} \tag{1}$$

where $R(x,y) = \frac{1}{N}\sum_{i=1}^{N}\sqrt{\frac{(x-x_i)^2+(y-y_i)^2}{-\log(f_{\mathrm{norm}}(x_i,y_i))}}$, N is the common candidate number, x and y indicate the leading candidate position, x_i and y_i describe the ith common candidate position, $f_{\mathrm{norm}}(\cdot)$ is the normalized objective function of the original optimal problem, $f_{\mathrm{o}}(\cdot)$ is the original objective function, and parameter β determines the relative importance of the robustness. We investigated the sensitivity of the proposed method to the β based on numerical tests. A large β leads to a relatively robust solution, while a small β corresponds to heavy reliance on the global (or local) optimal solution. Thus, we have developed a fitness evaluation function that balances the contribution of both optimal and robust evaluations according to the application of the robust optimization.

D. Update Candidate Pool (Step 4)

Since the local optimal solutions can also have the potential to be a robust one [14]. In this regard, we remove the leading candidate and all feasible particles except common candidate from the candidate pool, and find new $\mathrm{P_{lc}}$ from the particles that remained in the candidate pool. Steps 3–4 is repeated until the number of particles in the candidate pool is less than two since under this condition it is impossible to find common candidate.

E. Update Pbests, Gbests and Velocity (Step 5)

If the current fitness value is better than the old individual best value, the *pbest* is replaced by the current position. The old *gbest* is replaced by the best current *gbest* among the swarm if current *gbest* is better. The velocity of jth particle is updated based on (2) which is described clearly in [3] and [5]. Steps 2–5 are repeated until all particles are gathered around the *gbest*, or a maximum iteration is encountered.

$$\begin{aligned} Vx_j^{k+1} &= \omega \cdot Vx_j^k + C_p \cdot \varphi_p \cdot \left(pbestx_j^k - Px_j^k\right) \\ &\quad + C_g \cdot \varphi_g \cdot \left(gbestx_j^k - Px_j^k\right) \\ Vy_j^{k+1} &= \omega \cdot Vy_j^k + C_p \cdot \varphi_p \cdot \left(pbesty_j^k - Py_j^k\right) \\ &\quad + C_g \cdot \varphi_g \cdot \left(gbesty_j^k - Py_j^k\right) \end{aligned} \tag{2}$$

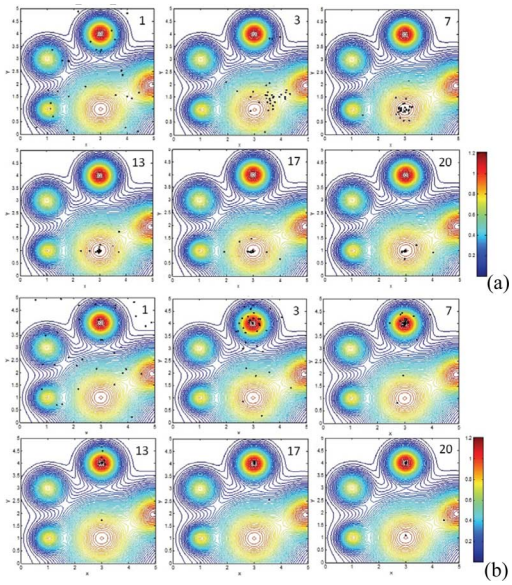

Fig. 3. The optimization result. (a) $\beta = 1$. (b) $\beta = 0$.

III. Numerical Test and Results

A 2-D mathematical function is used to verify the performance of the proposed algorithm formulated as

$$f(x,y) = \sum_{k=1}^{M} b_k \cdot e^{\frac{(x-x_{pk})^2+(y-y_{pk})^2}{-2\cdot a_k^2}} \tag{3}$$

where M is the total number of peaks. a_k and b_k are the width and amplitude of the kth peak. x_{pk} and y_{pk} are the position of the kth peak. x and y are the decision variables. The test function generated according to [8] is formulated as (4), the search space is $0 \le x, y \le 5$. Fig. 2 shows the shape of the test function, where total number of the optimal solution is 5 at positions (1,1), (1,3), (3,1), (3,4), and (5,2). The global optimal solution lies in position (3,4), the robust optimal solution is located at (3,1).

$$\begin{aligned} f(x,y) = {} & 0.7e^{\frac{(x-1)^2+(y-1)^2}{-0.18}} + 0.75e^{\frac{(x-1)^2+(y-3)^2}{-0.32}} + e^{\frac{(x-3)^2+(y-1)^2}{-2}} \\ & + 1.2e^{\frac{(x-3)^2+(y-4)^2}{-0.32}} + e^{\frac{(x-5)^2+(y-2)^2}{-0.72}} \end{aligned} \tag{4}$$

The conditions to execute the RPSO are defined as: number of iterations and particles are 20 and 36, ω is 0.6, $\mathrm{C_p}$ and $\mathrm{C_g}$ are 1.5. The optimization processes shown in Fig. 3(a) indicate that the RPSO can find robust optimal solution within 20 iterations, the number on the upper right corner is the iteration time. To observe the effect of the proposed method, we apply the RPSO by setting β value as 0 to the same test function and execution conditions. The result of the simulation is depicted in Fig. 3(b). The swarm converged to the global optimal solution due to the absence of the proposed robust evaluation of the solutions.

Next, we compare the performance between the proposed and conventional robust optimization methods from the standpoints of accuracy and computational costs. The conventional method means that the expected fitness function is determined from the

TABLE I
PERFORMANCES OF DIFFERENT METHODS ON THE TEST FUNCTION

Run number	Proposed method		Conventional method	
	Iterative number	Position (x, y)	Iterative number	Position (x, y)
1	97	**(3.0, 1.0)**	152	**(3.0, 1.0)**
2	108	**(3.0, 1.0)**	157	**(3.0, 1.0)**
3	116	**(3.0, 1.0)**	155	(3.0, 2.0)
4	148	**(3.0, 1.0)**	156	**(3.0, 1.0)**
5	164	(3.2, 1.1)	151	(4.9, 2.0)
6	85	**(3.0, 1.0)**	150	**(3.0, 1.0)**
7	97	**(3.0, 1.0)**	154	**(3.0, 1.0)**
8	135	**(3.0, 1.0)**	152	**(3.0, 1.0)**
9	51	**(3.0, 1.0)**	176	**(3.0, 1.0)**
10	148	**(3.0, 1.0)**	155	**(3.0, 1.0)**

formula (4) in [14]. The parameters and test function of two methods used for this comparison are same as given previously except the stop criterion. A method will stop its iterative process when the number of successive iterations without improvements in the best objective function so far searched reaches 50. Table I tabulates the performances of the proposed and conventional methods over 10 independent runs. It demonstrates higher success rate and lower computational costs of the proposed algorithm as compared to conventional one. Moreover, the failed solution (3.2, 1.1) from the proposed method is closer to the robust optimal solution (3.0, 1.0) than those (3.0, 2.0) and (4.9, 2.0) from the conventional method. From the comparison we can conclude that the merit of the proposed method is its high accuracy and low computational costs.

IV. APPLICATION TO THE ELECTROMAGNETIC PROBLEM

A. Objective Function and Design Variables

We demonstrate the efficiency and the performance of the proposed RPSO by applying it to an electromagnetic scattering problem [15]. It is an inverse design problem where the objective is to mimic a desired power distribution along the observation points by varying the dielectric region configurations. As shown in Fig. 4, a dielectric region is a subset of triangular meshes defined in the electromagnetic domain. Seed is the first triangular mesh selected to represent the dielectric region. In this paper, two seeds (two black triangles in Fig. 4) are restricted to locate in their respective orbits (two gray circles in Fig. 4), hence, the position of one seed can be determined by one design variable, i.e., the seed's degree in a specific orbit. In addition, we can grow the dielectric region by adding the closest triangular mesh (with respect to the seed) to the current dielectric region, or shrink the dielectric region by removing the furthest triangular mesh from the current dielectric region. So, the region extension can be determined by another variable, i.e., the number of triangular meshes inside the green region in Fig. 4. Teflon is modeled as a lossless dielectric with relative permittivity equals to 2.05. We assume there are two independent dielectric regions in the electromagnetic domain and each dielectric region is determined by two design variables This problem is a topology optimization in terms of searching seed positions, at the same time, it is also a shape optimization in terms of ascertaining region extensions.

The model is based on a 2-D homogeneous scalar wave equation for dielectric scatterers in conjunction with an absorbing boundary condition (ABC) [16]. Fig. 4 illustrates the setup of the domain, a TM^z uniform plane wave is incident upon a perfectly conducting circular cylinder of 0.5-wavelength radius.

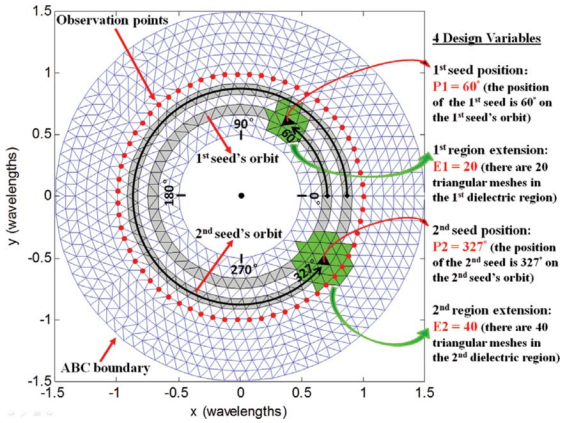

Fig. 4. The simulation layout showing the physical dimensions, triangular meshes and the definition of four design variables.

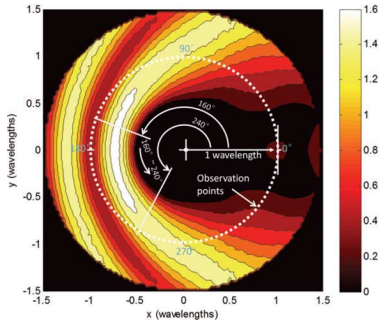

Fig. 5. Contour plot of the electric field.

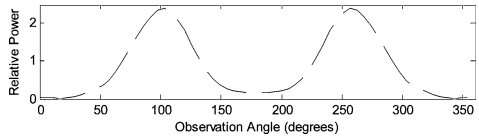

Fig. 6. The power distribution along the observation points.

The radial distance from the center of the cylinder to the observation points (white points in Fig. 5) is 1-wavelength whereas the radius of the ABC boundary is 1.5-wavelength. The finite element method is used to compute the field value [16]. Fig. 5 shows the contour plot of the relative magnitude of the electric field when there is no dielectric scatterer in the electromagnetic domain. The relative power distribution of the electric field along the observation points is shown in Fig. 6.

In the optimization problem, we seek to match the power profile $\mathbf{p}_{\mathrm{mod}}$ along the observation points to a desired power distribution $\mathbf{p}_{\mathrm{des}}$, which has a constant value 2 between 160° and 240° and is 0 everywhere else [the red line shown in Fig. 7(c)]. For any dielectric region configuration $\Re$, an objective function ζ measures the correlation coefficient of $\mathbf{p}_{\mathrm{mod}}$ and $\mathbf{p}_{\mathrm{des}}$ through

$$\zeta(\Re) = (\mathbf{p}_{\mathrm{mod}} \bullet \mathbf{p}_{\mathrm{des}}) \cdot (\|\mathbf{p}_{\mathrm{mod}}\|_2 \cdot \|\mathbf{p}_{\mathrm{des}}\|_2)^{-1} \qquad (6)$$

where $\bullet$ is the inner product, $\| \ \|_2$ is the standard L2-norm. ζ is -0.2213 when there is no dielectric scatterer.

B. Optimization Results

The left side of Fig. 7(a) is the optimized dielectric regions obtained by using the RPSO. The configuration includes four resulting design variables: two black points are the seed positions and two green area are the region extensions. The right side of

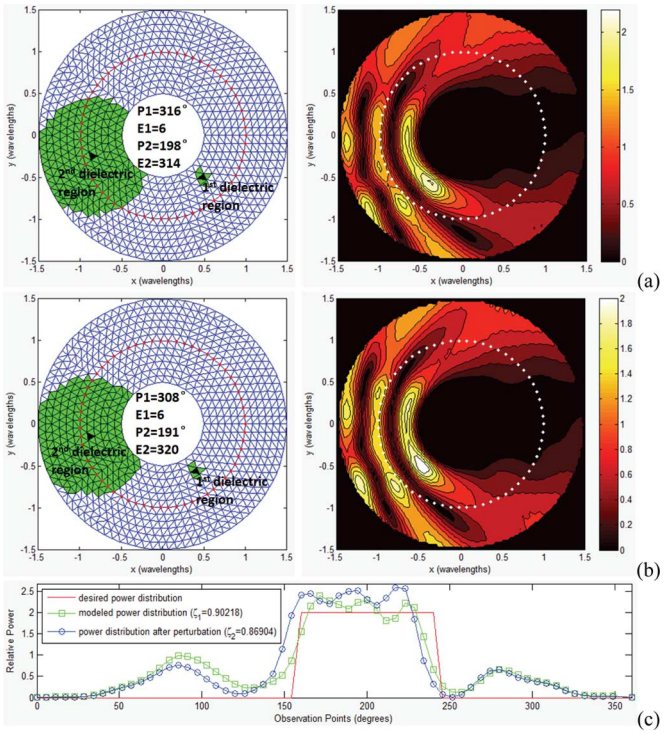

Fig. 7. The optimization result ($\beta = 0.3$). (a) The optimized dielectric regions and the modeled electric field. (b) The dielectric regions and the electric field after perturbation. (c) The desired (red), modeled (green) power distribution, and the power distribution after perturbation (blue).

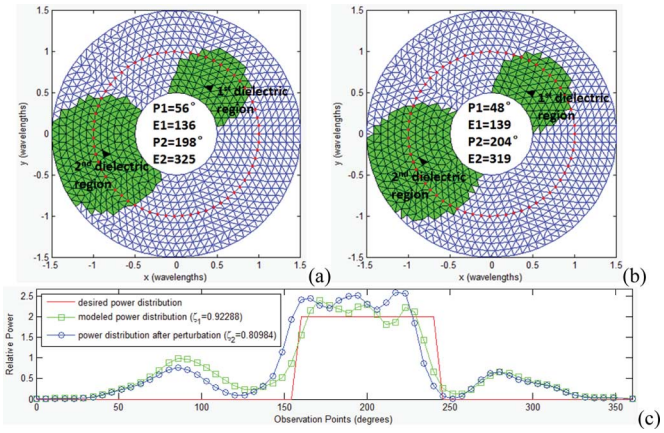

Fig. 8. The optimization result ($\beta = 0$). (a) The optimized dielectric regions. (b) The dielectric regions after perturbation. (c) The desired (red), modeled (green) power distribution, and the power distribution after perturbation (blue).

Fig. 7(a) is the modeled electric field, and the modeled power distribution ($\zeta_1 = 0.90218$) along the observation points is the green line in Fig. 7(c). The robustness of an optimal design is associated with performance degradation as a function of perturbation of the optimized topology and shape. Thereby, we add 2% perturbation to the optimized design variables, Fig. 7(b) shows the dielectric configuration and the electric field after perturbation, the power distribution ($\zeta_2 = 0.86904$) in this case is the blue line in Fig. 7(c). The performance degradation ratio is $|(\zeta_1 - \zeta_2)/\zeta_1| = 3.67\%$.

To observe an effect of the proposed expected fitness evaluation method on this electromagnetic problem, we apply the RPSO by setting β value as 0 under the same execution conditions. The result ($\zeta_1 = 0.92288, \zeta_2 = 0.80984$) is depicted in Fig. 8. The performance degradation ratio increases to 12.25%, more than 3 times the previous one (3.67%) due to the absence of the proposed robust evaluation. The optimization result is not robust against variation of design variables.

V. Conclusion

This paper proposed a PSO algorithm with novel expected fitness evaluation for robust optimization problems. Through the application to numerical function, it was revealed that the proposed PSO algorithm is promising for robust optimization problems. Moreover, the validity of the proposed algorithm was also tested by the electromagnetic scattering problem. The results confirmed that the dielectric configuration obtained by the proposed PSO showed stronger robustness against design variable errors than that by the general purpose PSO. The beta is important to consider the robustness of objective functions and the uncertainty in design variables, especially in practical equipment or device design. Thus, to enable the proposed approach to become a powerful and widely recognized robust optimizer, we will further investigate the relationship between the manufacturing error and the parameter beta, then add this information into the proposed method in the future.

References

[1] J. Kennedy and R. Eberhart, "Particle swarm optimization," in *Proc. IEEE Int. Conf. Neural Netw.*, 1995, vol. 4, pp. 1942–1948.

[2] S. Sumathi and P. Surekha, *Computational Intelligence Paradigms Therory and Applications Using Matlab*. Boca Raton, FL: CRC Press, 2010, pp. 656–671.

[3] J. H. Seo, C. H. Im, C. G. Heo, J. K. Kim, H. K. Jung, and C. G. Lee, "Multimodal function optimization based on particle swarm optimization," *IEEE Trans. Magn.*, vol. 42, no. 4, pp. 1095–1098, Apr. 2006.

[4] M. Azab, "Harmonic elimination in three-phase voltage source inverters by particle swarm optimization," *J. Electr. Eng. Technol.*, vol. 6, no. 3, pp. 334–341, 2011.

[5] J. H. Seo, C. H. Im, S. Y. Kwak, C. G. Lee, and H. K. Jung, "An improved particle swarm optimization algorithm mimicking territorial dispute between groups for multimodal function optimization problems," *IEEE Trans. Magn.*, vol. 44, no. 6, pp. 1046–1049, Jun. 2008.

[6] C. Venkaiah and D. M. V. Kumar, "Fuzzy PSO congestion management using sensitivity-based optimal active power rescheduling of generateors," *J. Electr. Eng. Technol.*, vol. 6, no. 1, pp. 32–41, 2011.

[7] A. Ajami, G. Aghajani, and M. Pourmahmood, "Optimal location of FACTS devices using adaptive particle swarm optimization hybrid with simulated annealing," *J. Electr. Eng. Technol.*, vol. 5, no. 2, pp. 179–190, 2010.

[8] S. L. Ho, S. Yang, G. Ni, and K. W. E. Cheng, "An efficient Tabu search algorithm for robust solutions of electromagnetic design problems," *IEEE Trans. Magn.*, vol. 44, no. 6, pp. 1042–1047, Jun. 2008.

[9] S. L. Ho and S. Yang, "A population-based incremental learning method for robust optimal solutions," *IEEE Trans. Magn.*, vol. 46, no. 8, pp. 3189–3192, Aug. 2010.

[10] H. G. Beyer and B. Sendhoff, "Robust optimization—A comprehensive survey," *Comput. Methods Appl. Mech. Eng.*, vol. 196, pp. 3190–3218, 2007.

[11] J. H. Ko, J. K. Byun, J. S. Park, and H. S. Kim, "Robust design of dual band/polarization patch antenna using sensitivity analysis and Taguchi's method," *IEEE Trans. Magn.*, vol. 47, no. 5, pp. 1258–1261, May 2011.

[12] D. Bertsimas, O. Nohadani, and K. M. Teo, "Robust optimization in electromagnetic scattering problems," *J. Appl. Phys.*, vol. 101, no. 7, pp. 0745071–0745077, Apr. 2007.

[13] D. Bertsimas and O. Nohadani, "Robust optimization with simulated annealing," *J. Global Optim.*, vol. 48, no. 2, pp. 323–334, Oct. 2010.

[14] S. L. Ho, S. Yang, Y. Yao, and W. N. Fu, "Robust optimization using a methodology based on cross entropy methods," *IEEE Trans. Magn.*, vol. 47, no. 5, pp. 1286–1289, May 2011.

[15] P. Seliger, M. Mahvash, C. Wang, and A. F. J. Levi, "Optimization of aperiodic dielectric structure," *J. Appl. Phys.*, vol. 100, no. 3, pp. 0343101–0343106, Aug. 2006.

[16] A. C. Polyearpou, *Introduction to the Finite Element Method in Electromagnetic*. San Rafael, CA: Morgan & Claypool, 2006, pp. 97–105.